Ganpat University
॥ विद्यया समाजोत्कर्षः ॥

University Journal of Research
ISSN (Online) 2455-1724

Magnetic field and Heat generation effects on two phases blood flow in stenosed artery

Harshad Patel[a], Nilesh Patel[b]

[a]*U.V.P.C.E.,Ganpat University, Kherva, Gujarat – 384012, India*
[b]*B.S.P.P,Ganpat University, Kherva, Gujarat – 384012, India.*

Abstract

This study investigates the effects of heat generation and magnetic fields on two-phase blood flow in a stenosed artery, focusing on the distinct regions of the core and plasma. The governing mathematical model comprises a system of partial differential equations (PDEs) that are transformed into a system of ordinary differential equations (ODEs) through similarity transformations. Analytical solutions for the velocity, temperature, and concentration profiles in both regions are derived using Bessel's equation. To enhance the understanding of the underlying physics, numerical simulations are conducted, and the results are presented graphically. The findings indicate that the presence of a magnetic field significantly reduces blood motion in both the core and plasma regions. This research contributes to the understanding of hemodynamic behavior in pathological conditions, with implications for the development of therapeutic strategies targeting arterial diseases.

Keywords:- Heat Transfer; Stenosed Artery; Blood Flow; Magnetic Field; Heat generation; Bessel Function.

1. Introduction

Blood flow dynamics in arteries can be significantly altered by conditions such as aneurysms and stenosis. Arteriosclerosis, commonly known as stenosis, involves the narrowing of arteries due to plaque buildup and inflammatory processes. This vascular condition results from various factors, including lipid deposits within arterial walls and changes in tissue pathology [1-2]. Researchers have suggested that hydrodynamic factors could play a crucial role in understanding a variety of vascular diseases [3]. For example, Clark [4] conducted experiments with different stenosis models, revealing that as stenosis progresses, the arterial diameter experiences substantial reduction. The study of blood flow dynamics (BFD) in conjunction with magnetic fields has attracted significant interest due to its potential therapeutic applications [5-6]. Tzirtzilkis [7] explored how bio-magnetic fluid (blood) circulation can be regulated through constricted pathways under the influence of magnetic fields. Ponalagusamy and Selvi [8] investigated the effects of magnetic fields and heat transfer on two-phase blood flow models, employing both one-phase and two-phase models to evaluate the impact of magnetization [9]. Their research highlighted critical factors, such as lower shear stress on arterial walls and variations in longitudinal impedance and plug core radius. Magnetohydrodynamics (MHD) is the study of electrically conducting fluid flow within magnetic fields [10]. In a related study, Ali et al. [11] analyzed MHD blood flow by modeling blood as a Casson fluid, concluding that magnetic exposure reduces both blood and magnetic particle movement. Ponalagusamy and Selvi [12] further examined heat transfer in MHD two-phase blood flow systems. Misra et al. [13] developed a model treating the artery as a conduit, finding that the strength of an applied magnetic field can be adjusted to manipulate blood flow rates. Majee and Shit [14] studied the impact of heat transfer on MHD blood flow in stenosed arteries, revealing that an increase in the magnetic field parameter raises blood flow temperature, a finding that has implications for tumor hyperthermia [15]. Recent advancements have emphasized the use of computational fluid dynamics (CFD) to gain insights into blood flow in diseased arteries, allowing for more accurate modeling of complex flow behaviors and aiding in predicting disease progression [16-17]. Additionally, advanced imaging technologies, including MRI and ultrasound, have enhanced our understanding of blood flow distribution, providing valuable insights into hemodynamic changes associated with stenosis [18-19].

*Corresponding Author
E-mail address: nmp01@ganpatuniversity.ac.in

This study aims to deepen the understanding of the interplay between arterial wall biology, biomechanics, and geometric factors by examining yield stress, stenosis height, and the effects of magnetic fields. By addressing these factors, we can improve our understanding of arterial diseases and their biomechanics, contributing to better diagnostic and therapeutic strategies [20-21]. Furthermore, the role of temperature in blood viscosity has been a topic of considerable interest. In two-phase blood flow models, the core region's viscosity varies with temperature, while the viscosity of the plasma remains constant throughout the process [22-23]. The governing non-linear partial differential equations were solved using the Bessel equation, demonstrating two-phase blood flow through a stenosed artery and illustrating the influence of varying parameters on flow properties [24-25]. By employing a two-fluid model, researchers such as Ikbal et al. [26] and Ponalagusamy [27] have assessed the flow properties of blood, comparing their findings with experimental data. Understanding these properties is crucial for developing strategies to mitigate the effects of stenosis and other vascular diseases [28-29]. Ultimately, the findings from this research are expected to provide insights into the mechanics of arterial disease and aid in the development of innovative treatment approaches that enhance patient outcomes [30].

In the two-phase flow of blood, the viscosity of the core area is temperature-dependent, whereas the viscosity of the plasma region is viewed as constant throughout the process. The Bessel equation was utilised to provide a solution for the governing non-linear partial differential equations. Two-phase blood flow through a stenosed artery is shown graphically, along with the impact of varying parameters on the flow's properties.

The link between artery wall biology, biomechanics, and geometric difficulties may be understood by studying yield stress, stenosis height, and magnetic field. This study helps interpret arterial disease and biomechanics.

Nomenclature:

$\overline{B_0}$	Magnetic field intensity
$\overline{L_0}$	length of stenosis
$\bar{d}$	location of artery
β	central core radius and normal artery radius ratio.
$\beta\overline{R_0}$	Normal artery core region radius
n	Shape of the constriction profile
$\overline{D}$	Coefficient of mass diffusivity
$\frac{\partial \bar{p}}{\partial \bar{z}}$	Pressure gradient

$\bar{c}$	specific heat
$\bar{u}$	Velocity
$\overline{T}$	Temperature
$\bar{C}$	Concentration
$\overline{K}$	Thermal conductivity
$\bar{\sigma}$	Electrical conductivity
$\bar{\rho}$	Density

2. Mathematical Modelling

Consider unsteady blood flow of axially symmetric two-phase model with core region radius $\overline{R_1}\,(\bar{z})$, plasma region radius $\bar{R}\,(\bar{z})$ and cylindrical stenosed artery radius $\overline{R_0}$ which is describe in Figure 1. The blood flow considered in stenosis artery with magnetic field. The field is applied in perpendicular which is shown in Figure 1. The $(\overline{u_c}, \overline{v_c}, \overline{w_c})$ and $(\overline{u_p}, \overline{v_p}, \overline{w_p})$ are velocity expression for core and plasma regions respectively along with $(\bar{r}, \bar{\theta}, \bar{z})$ directions in the cylindrical coordinates. The temperature and concentration near the walls are assumed $\overline{T_w}$ and $\overline{C_w}$ respectively.

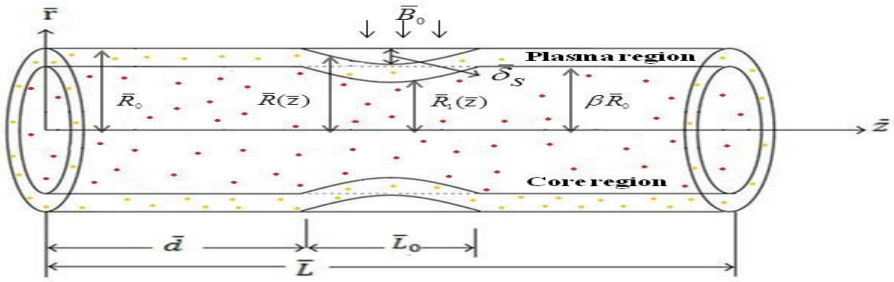

Figure 1. Physical Sketch

The blood flow viscosities of both regions can be written as,

$$\bar{\mu}(\bar{r}) = \begin{cases} \overline{\mu_c} & for \quad 0 \le r \le \overline{R_1}(\bar{z}) \\ \overline{\mu_p} & for \quad \overline{R_1}(\bar{z}) \le r \le \bar{R}(\bar{z}) \end{cases} \tag{1}$$

The representation of stenosis for both regions are defined as,

$$\frac{\bar{R}(\bar{z})}{\overline{R_0}} = \begin{cases} 1 - \frac{\overline{\delta_s} n^{\frac{n}{n-1}}}{\overline{R_0}\,\overline{L_0}^{n}(n-1)} \left(\overline{L_0}^{n-1}\left(\bar{z}-\bar{d}\right) - \left(\bar{z}-\bar{d}\right)^n \right) & for \quad \bar{d} \le \bar{z} \le \bar{d} + \overline{L_0} \\ 1, & Otherwise \end{cases} \tag{2}$$

$$\frac{\bar{R}(\bar{z})}{\overline{R_0}} = \begin{cases} \beta - \frac{\overline{\delta_s} n^{\frac{n}{n-1}}}{\overline{R_0}\,\overline{L_0}^{n}(n-1)} \left(\overline{L_0}^{n-1}\left(\bar{z}-\bar{d}\right) - \left(\bar{z}-\bar{d}\right)^n \right) & for \quad \bar{d} \le \bar{z} \le \bar{d} + \overline{L_0} \\ \beta, & Otherwise \end{cases} \tag{3}$$

Now, under the all assumptions, velocity, temperature and concentration for core region are as follows,

$$\overline{\rho_c}\frac{\partial \overline{u_c}}{\partial \bar{t}} = -\frac{\partial \bar{p}}{\partial \bar{z}} + \overline{\mu_c}\left(\frac{\partial^2 \overline{u_c}}{\partial r^2} + \frac{1}{r}\frac{\partial \overline{u_c}}{\partial r}\right) - \sigma . B_0^2 \overline{u_c} \tag{4}$$

$$\overline{\rho_c}\,\overline{C_c}\frac{\partial \overline{T_c}}{\partial \bar{t}} = \overline{K_c}\left(\frac{\partial^2 \overline{T_c}}{\partial r^2} + \frac{1}{r}\frac{\partial \overline{T_c}}{\partial r}\right) + (T_c - T_\infty) \tag{5}$$

Similarly, for plasma region are given by

$$\overline{\rho_p}\frac{\partial \overline{u_p}}{\partial \bar{t}} = -\frac{\partial \bar{p}}{\partial \bar{z}} + \overline{\mu_p}\left(\frac{\partial^2 \overline{u_p}}{\partial r^2} + \frac{1}{r}\frac{\partial \overline{u_p}}{\partial r}\right) - \sigma . B_0^2 \overline{u_p} \tag{6}$$

$$\overline{\rho_p}\,\overline{C_p}\frac{\partial \overline{T_p}}{\partial \bar{t}} = \overline{K_c}\left(\frac{\partial^2 \overline{T_p}}{\partial r^2} + \frac{1}{r}\frac{\partial \overline{T_p}}{\partial r}\right) + (T_p - T_\infty) \tag{7}$$

In equations (4) - (7), subscripts c and p stand for core and plasma regions respectively.

The appropriate boundary conditions for the model under consideration are as follows:

$$\overline{\mu_p} = 0, \qquad T_p = T_w, \quad at \ \bar{r} = \bar{R}(\bar{z})$$

$$\overline{\mu_c} = \overline{\mu_p}, \qquad T_p = T_c, \quad at \ \bar{r} = \overline{R_1}(\bar{z}),$$

$$\frac{\partial \overline{q_c}}{\partial r} = 0, \qquad \frac{\partial \overline{T_c}}{\partial r} = 0, \qquad at \ \bar{r} = 0,$$

$$T_c = T_p, \qquad \frac{\partial \overline{T_c}}{\partial r} = \frac{\partial \overline{T_p}}{\partial r}, \quad at \ \bar{r} = \overline{R_1}(\bar{z}) \tag{8}$$

Now, we introduce the following dimensionless parameters:

$$u_c = \frac{\overline{u_c}}{\overline{u_0}}, \ r = \frac{\bar{r}}{\overline{R_0}}, t = \overline{\omega}\,\bar{t}, \ R(z) = \frac{\bar{R}(\bar{z})}{\overline{R_0}}, D_0 = \frac{\overline{D_p}}{\overline{D_c}}, p = \frac{\overline{R_0}\bar{p}}{\overline{\mu_0}\overline{\mu_p}}, \delta = \frac{\overline{\delta_s}}{\overline{R_0}}, \ \theta_c = \frac{(T_c - T_0)}{(T_w - T_0)},$$

$$u_c = \frac{\overline{\mu_c}}{\overline{\mu_0}}, \theta_p = \frac{(T_p - T_0)}{(T_w - T_0)}, \mu_0 = \frac{\overline{\mu_p}}{\overline{\mu_c}}, \ M^2 = \frac{\varphi \overline{R_0}^2 \overline{B_0}^2}{\overline{\mu_p}}, \quad P_e = \frac{\overline{\rho_p}\,\overline{C_p}\,\overline{R_0}^2 \omega}{\overline{k_p}}, \rho_0 = \frac{\overline{\rho_p}}{\overline{\rho_c}}$$

For core region Equations (4) - (5), dimensionless form can be express as

$$\left(\frac{Re}{\rho_0}\right)\frac{\partial u_c}{\partial t} = -\frac{\partial p}{\partial z} + \frac{1}{\mu_0}\left(\frac{\partial^2 u_c}{\partial r^2} + \frac{1}{r}\frac{\partial u_c}{\partial r}\right) - M^2 u_c \tag{9}$$

$$\frac{P_e K_0}{\rho_0 s_0}\left(\frac{\partial \theta_c}{\partial t}\right) = \left(\frac{\partial^2 \theta_c}{\partial r^2} + \frac{1}{r}\frac{\partial \theta_c}{\partial r}\right) + H\,\theta_c \tag{10}$$

For plasma region Equations (6) - (7), dimensionless form can be express as

$$\left(\frac{Re}{\rho_0}\right)\frac{\partial u_p}{\partial t} = -\frac{\partial p}{\partial z} + \frac{1}{\mu_0}\left(\frac{\partial^2 u_p}{\partial r^2} + \frac{1}{r}\frac{\partial u_p}{\partial r}\right) - M^2 u_p \tag{11}$$

$$P_e\left(\frac{\partial \theta_p}{\partial t}\right) = \left(\frac{\partial^2 \theta_p}{\partial r^2} + \frac{1}{r}\frac{\partial \theta_p}{\partial r}\right) + H\,\theta_c \tag{12}$$

Similarly, the corresponding boundary conditions equation (10) in dimensionless form are given as

$$\begin{aligned} &u_p = 0, \quad \theta_p = 1, \quad at\ r = R(z) \\ &u_p = u_c, \quad \theta_p = \theta_c, \quad at\ r = R_1(z), \\ &T_c = T_p, \quad \frac{\partial \theta_c}{\partial r} = \frac{\partial \theta_p}{\partial r}, \quad at\ \ r = R_1(z), \\ &\frac{\partial u_c}{\partial r} = 0, \quad \frac{\partial \theta_c}{\partial r} = 0, \quad at\ \ r = 0 \end{aligned} \tag{13}$$

3. Solution of the Problem

In the blood flow, it is considered pressure gradient which can be represent as,

$-\frac{\partial p}{\partial z} = P_o e^{i\omega t}$, where, P_o represent the constant pressure.

As equations (9) to (13) are linear, the expression of all profiles can be written as,

$$u_c(r,t) = u_{c_0}(r)\, e^{i\omega t}, \quad u_p(r,t) = u_{p_0}(r) e^{i\omega t}, \tag{14}$$

$$\theta_c(r,t) = \theta_{c_0}(r)\, e^{i\omega t}, \quad \theta_p(r,t) = \theta_{p_0}(r)\, e^{i\omega t}, \tag{15}$$

Now, using equation (14), equations (9) - (10) can be converted in the form of

$$\left(\frac{\partial^2 u_{c_0}}{\partial r^2} + \frac{1}{r}\frac{\partial u_{c_0}}{\partial r}\right) - \left(M^2 + \frac{\mu_c Re}{\rho_0}\, i\right) u_{c_0} = -P_0\mu_0 \tag{16}$$

$$\left(\frac{\partial^2 \theta_{c_0}}{\partial r^2} + \frac{1}{r}\frac{\partial \theta_{c_0}}{\partial r}\right) - \left(i\,\frac{P_e K_0}{\rho_0 s_0} - H\right)\theta_{c_0} = 0 \tag{17}$$

Similarly, substituting equation (14) into equations (11) - (12), we get

$$\left(\frac{\partial^2 u_{p_0}}{\partial r^2} + \frac{1}{r}\frac{\partial u_{p_0}}{\partial r}\right) - (M^2 + Re\, i) u_{p_0} = -P_0 \tag{18}$$

$$\left(\frac{\partial^2 \theta_{p_0}}{\partial r^2} + \frac{1}{r}\frac{\partial \theta_{p_0}}{\partial r}\right) - (i\,P_e - H)\theta_{p_0} = 0 \tag{19}$$

To find the exact expression of temperature profiles for core and plasma region, applying Bessel's differential equations on (17) and (19) with boundary conditions (14),

For simplicity, Assume the following term as,

So, the equations and change in form of

$$\left(\frac{\partial^2\theta_{c_0}}{\partial r^2}+\frac{1}{r}\frac{\partial\theta_{c_0}}{\partial r}\right)-{A_1}^2\theta_{c_0}=0 \tag{20}$$

$$\left(\frac{\partial^2\theta_{p_0}}{\partial r^2}+\frac{1}{r}\frac{\partial\theta_{p_0}}{\partial r}\right)-{A_2}^2\theta_{p_0}=0 \tag{21}$$

Where,

$${A_1}^2=-\left(i\,\frac{P_e K_0}{\rho_0 s_0}-H\right) \tag{22}$$

$${A_2}^2=-(i\,P_e-H) \tag{23}$$

Now, the exact solution of energy equation of core as well as plasma regions respectively, are

$$\theta_{c_0}=\left[X_1\left(\frac{A_2Y_1(A_2R_1)}{X_4Y_0(A_2R)}-\frac{A_1J_1(A_1R_1)}{X_4}+X_2\right)\right]J_0(A_1r) \tag{24}$$

$$\theta_{p_0}=\left[\left(\frac{A_2Y_1(A_2R_1)}{X_4Y_0(A_2R)}-\frac{A_1X_2J_1(A_1R_1)}{X_4}\right)\left(J_0(A_2r)-\frac{J_0(A_2R)}{Y_0(A_2R)}Y_0(A_2r)\right)\right]+\frac{Y_0(A_2r)}{Y_0(A_2R)} \tag{25}$$

Where,

$$X_1=\frac{J_0(A_2R_1)}{J_0(A_1R_1)}-\frac{J_0(A_2R)}{Y_0(A_2R)}.\frac{Y_0(A_2R_1)}{J_0(A_1R_1)},\ X_2=\frac{Y_0(A_2R_1)}{J_0(A_1R_1)Y_0(A_2R)} \tag{26}$$

$$X_3=J_1(A_2R_1)-\frac{J_0(A_2R)}{Y_0(A_2R)}Y_1(A_2R_1),\ X_4=A_1X_1J_1(A_1R_1)-A_2X_3 \tag{27}$$

Where, $J_n(x)$ and $Y_n(x)$ are the Bessel's function of first and second kind for integer value of n. The expressions of temperature for both regions, are as follows

$$\theta_c(r,t)=\left\{\left[X_1\left(\frac{A_2Y_1(A_2R_1)}{X_4Y_0(A_2R)}-\frac{A_1J_1(A_1R_1)}{X_4}+X_2\right)\right]J_0(A_1r)\right\}e^{i\omega t} \tag{28}$$

$$\theta_p(r,t)=\left[\left(\frac{A_2Y_1(A_2R_1)}{X_4Y_0(A_2R)}-\frac{A_1X_2J_1(A_1R_1)}{X_4}\right)\left(J_0(A_2r)-\frac{J_0(A_2R)}{Y_0(A_2R)}Y_0(A_2r)\right)\right]e^{i\omega t}+\frac{Y_0(A_2r)}{Y_0(A_2R)}e^{i\omega t} \tag{29}$$

We consider that

$$\left(\frac{\partial^2u_{c_0}}{\partial r^2}+\frac{1}{r}\frac{\partial u_{c_0}}{\partial r}\right)+{P_1}^2u_{c_0}=-P_0\mu_0, \text{ where } \quad {P_1}^2=-\left(M^2+\frac{\mu_c R e}{\rho_0}\,i\right) \tag{30}$$

The complementary solution for velocity profile is

$$u_{c_{0c}}=C_1J_0(P_1r)+C_2Y_0(P_1r) \tag{31}$$

Where, $u_{c_{01}}=J_0(P_1r)$ and $u_{c_{02}}=Y_0(P_1r)$ (32)

The Wronskian of these two functions is

$$W_1=\begin{vmatrix} J_0(P_1r) & Y_0(P_1r) \\ -P_1J_1(P_1r) & -P_1Y_1(P_1r)\end{vmatrix}=\frac{2}{\pi r} \tag{33}$$

The complete solution of equation (28), we have to find out

$$N_1=-\int\frac{Y_0(P_1r)P_0\mu_0}{W_1}\,dr\ \&\ M_1=-\int\frac{J_0(P_1r)P_0\mu_0}{W_1}\,dr \tag{34}$$

For the core region, the complete solution of velocity profile is given as,

$$u_{c_0}=C_1J_0(P_1r)+C_2Y_0(P_1r)+N_1J_0(P_1r)+M_1Y_0(P_1r) \tag{35}$$

For plasma region, we assume that

$$P_2^{\,2} = -(M^2 + Re\, i) \tag{36}$$

So the equation (18) becomes,

$$\frac{\partial^2 u_{p_0}}{\partial r^2} + \frac{1}{r}\frac{\partial u_{p_0}}{\partial r} - P_2^{\,2} u_{p_0} = -P_0 \tag{37}$$

Similarly, the complementary solution for velocity profile as,

$$u_{p_{0c}} = C_3 J_0(P_2 r) + C_4 Y_0(P_2 r) \tag{38}$$

Where, $u_{p_{01}} = J_0(P_2 r)$ and $u_{p_{02}} = Y_0(P_2 r)$ (39)

The Wronskian of these two functions is

$$W_2 = \begin{vmatrix} J_0(P_2 r) & Y_0(P_2 r) \\ -P_2 J_1(P_2 r) & -P_2 Y_1(P_2 r) \end{vmatrix} = \frac{2}{\pi r} \tag{40}$$

To find the complete solution of the non-homogeneous equation (37), first we have to find out

$$N_2 = -\int \frac{Y_0(P_2 r)\, P_0 \mu_0}{W_2}\, dr \;\; \& \;\; M_2 = -\int \frac{J_0(P_2 r)\, P_0 \mu_0}{W_2}\, dr \tag{41}$$

For the core region, the complete solution of velocity profile is given as,

$$u_{p_0} = C_3 J_0(P_2 r) + C_4 Y_0(P_2 r) + N_2 J_0(P_2 r) + M_2 Y_0(P_2 r) \tag{42}$$

After applying the boundary conditions equation (13) into equation (35) and equation (42),

We get $\frac{\partial u_c}{\partial r} = 0 \; at \; r = 0 \Rightarrow C_2 = 0$ (43)

Now, equation (50) becomes

$$u_{c_0} = C_1 J_0(P_1 r) + N_1 J_0(P_1 r) + M_1 Y_0(P_1 r) \tag{44}$$

After applying all the boundary condition, we obtain a linear system of $C_1, C_3 \; and \; C_4$ in the form of

$$\begin{bmatrix} J_0(P_1 R_1) & -J_0(P_2 R_1) & Y_0(P_2 R_1) \\ 0 & J_0(P_2 R) & Y_0(P_2 R) \\ P_1 J_1(P_1 R_1) & P_2 J_1(P_2 R_1) & P_2 Y_1(P_2 R_1) \end{bmatrix} \begin{bmatrix} C_1 \\ C_3 \\ C_4 \end{bmatrix} = \begin{bmatrix} D_1 \\ D_3 \\ D_4 \end{bmatrix} \tag{45}$$

Where, $D_1, D_3 \; and \; D_4$ are expressed as

$$D_1 = A_1 R_1 J_0(P_1 R_1) - B_1 R_1 Y_0(P_1 R_1) + A_2 R_1 J_0(P_2 R_1) + B_2 R_1 Y_0(P_2 R_1) \tag{46}$$

$$D_3 = -A_2 R\, J_0(P_2 R) + B_2 R\, Y_0(P_2 R) \tag{47}$$

$$D_4 = -\frac{\partial A_1 R_1}{\partial r} J_0(P_1 R_1) + A_1 R_1 P_1 Y_1(P_1 R_1) - \frac{\partial B_1 R_1}{\partial r} Y_0(P_1 R_1) - B_1 R_1 P_1 Y_1(P_1 R_1) + \frac{\partial A_2 R_1}{\partial r} J_0(P_2 R_1) + \frac{\partial B_2 R_1}{\partial r} Y_0(P_2 R_1) - P_2 A_2 R_1 J_1(P_2 R_1) + B_2 R_1 P_2 Y_1(P_2 R_1) \tag{48}$$

Equation (45) is a system of linear system with C_1, C_3 and C_4 are unknowns. So, the obtained the unique solutions of this system and substituting the values of C_1, C_3 and C_4 in equations (42) and (44).

Where, $\tau = \frac{\partial u_c}{\partial r}$ – inter face wall of the shear stress and $\tau' = \frac{1}{u_0}\frac{\partial u_p}{\partial r}$ – outer wall shear stress.

∴ The total volumetric flow rate Q_c and Q_p of blood flow for both regions in the artery is defined as

$$Q_c = 2\pi R^2 \int_0^K u_c(r,t)\, dr \quad \text{and} \quad Q_p = 2\pi R^2 \int_{R_1}^K u_p(r,t)\, dr \tag{49}$$

The total volumetric flow rate Q is given as

$$Q = Q_c + Q_p$$

$$= 2\pi R^2 \int_0^K u_c(r,t)\, dr + 2\pi R^2 \int_{R_1}^K u_p(r,t)\, dr \tag{50}$$

With the help of the equations (42) and (44), we can find analytic expression for the volumetric flow rate Q.

4. Results and discussion

The better understanding of the said problems, numerical solution is obtained and express through the Fig. 2 to 13. In all figures the core region radial distance is considered 0 to 0.7 where plasma region 0.7 to 0.9.

Figures 2 and 3 depict the velocity profiles for both regions under varying viscosity parameters. In both cases, an increase in the viscosity parameter correlates with an upward trend in velocity profiles. Figures 4 and 5 illustrate the influence of Reynolds number on velocity profiles. It is observed that as Reynolds number increases, the velocity of the fluid decreases. Near the tube wall, the velocity decreases significantly compared to near the axis, where it remains relatively unchanged. As we proceed along the radial distance from the axis of the tube, we see that the velocity remains virtually unchanged; but, as we get closer to the wall, it begins to slow down.

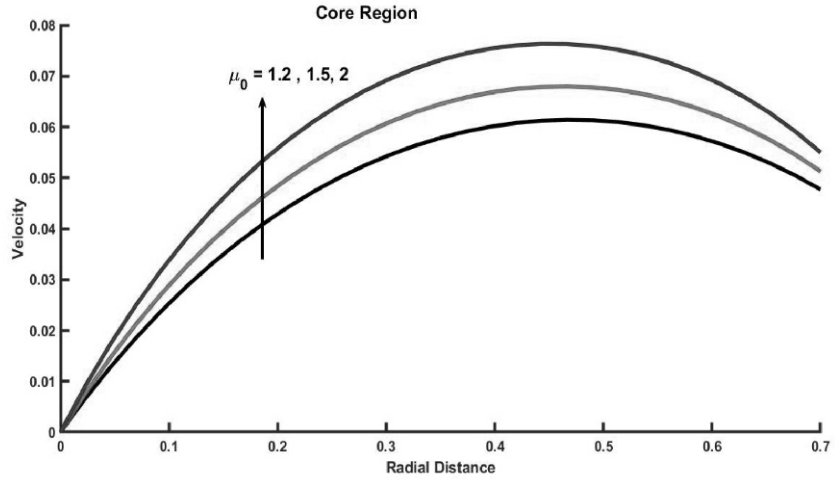

Fig. 2: velocity for μ_0

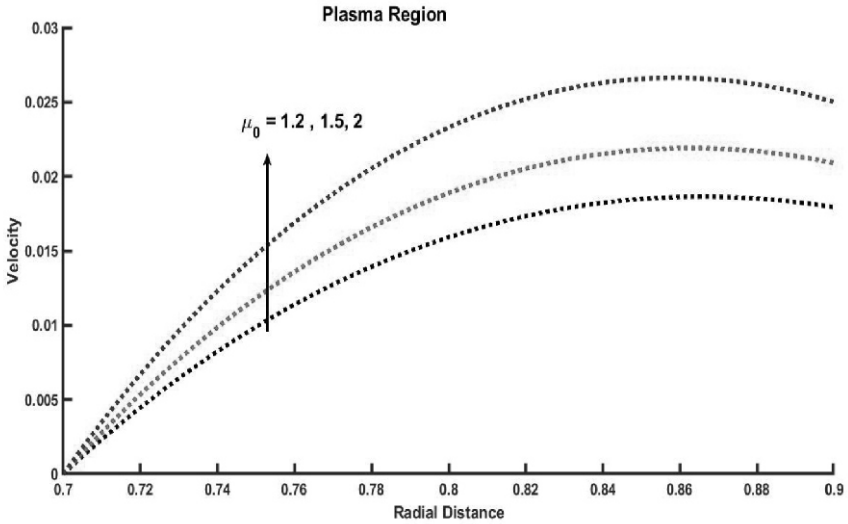

Fig. 3: velocity for μ_0

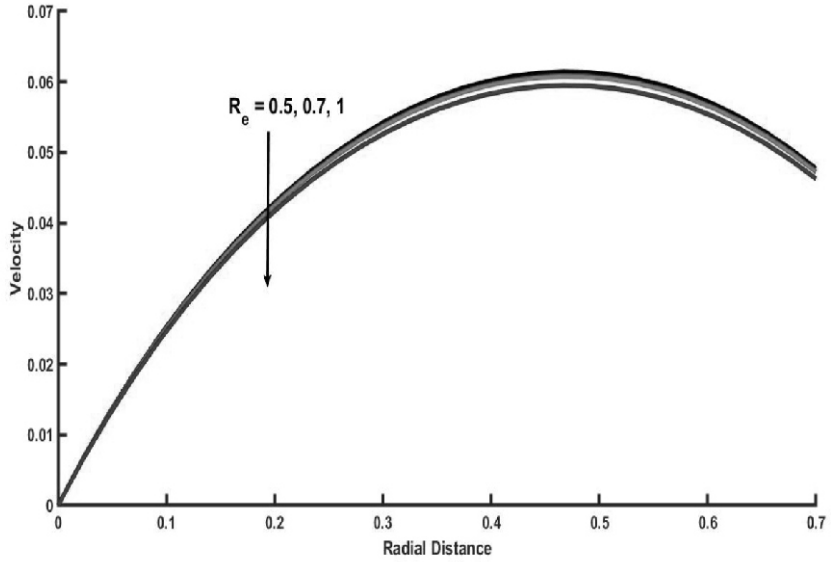

Fig. 4: Velocity for R_e.

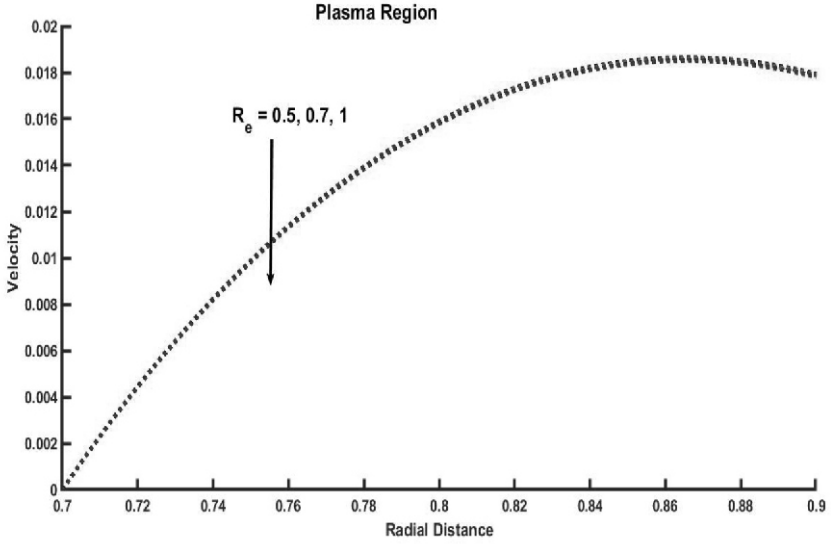

Fig. 5: Velocity for R_e.

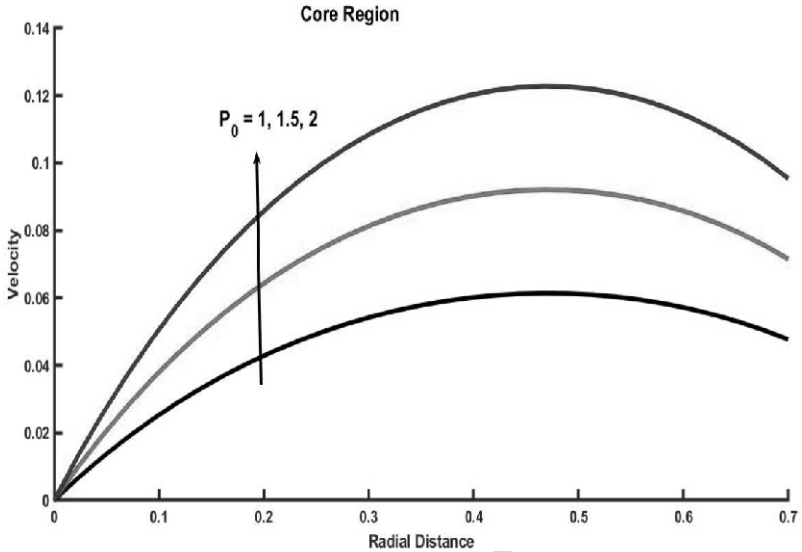

Fig. 6: Velocity for P_0.

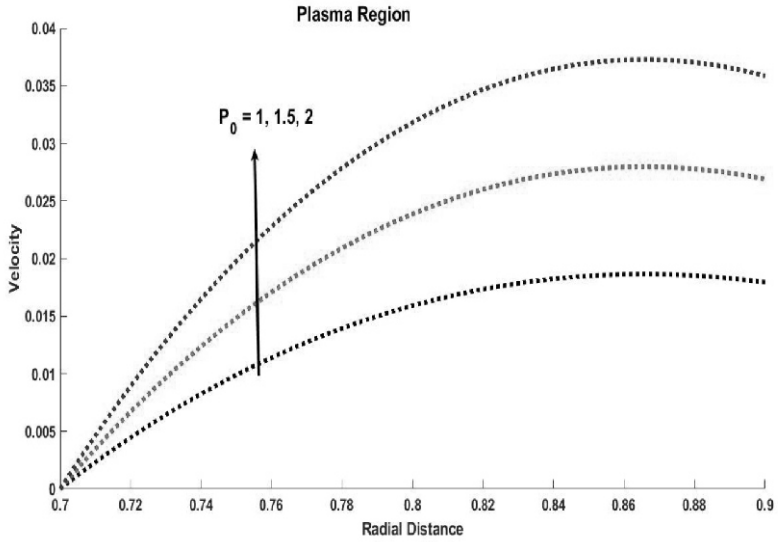

Fig. 7: Velocity for P_0.

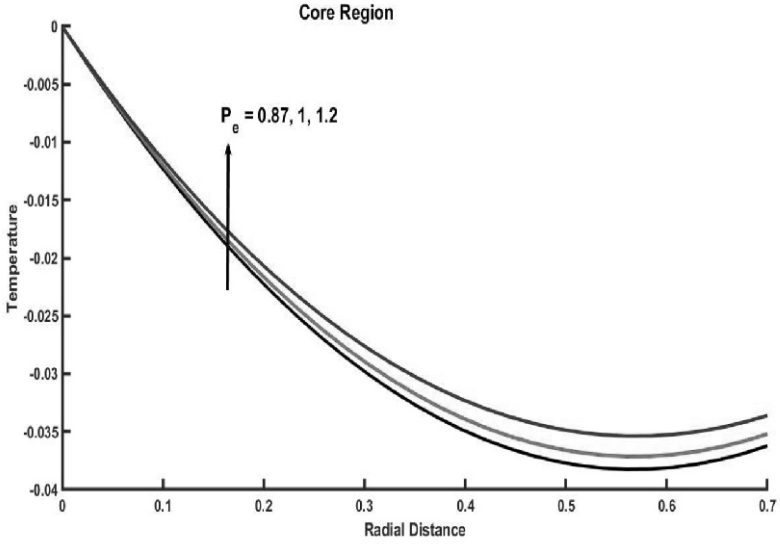

Fig. 8: Temperature for P_e.

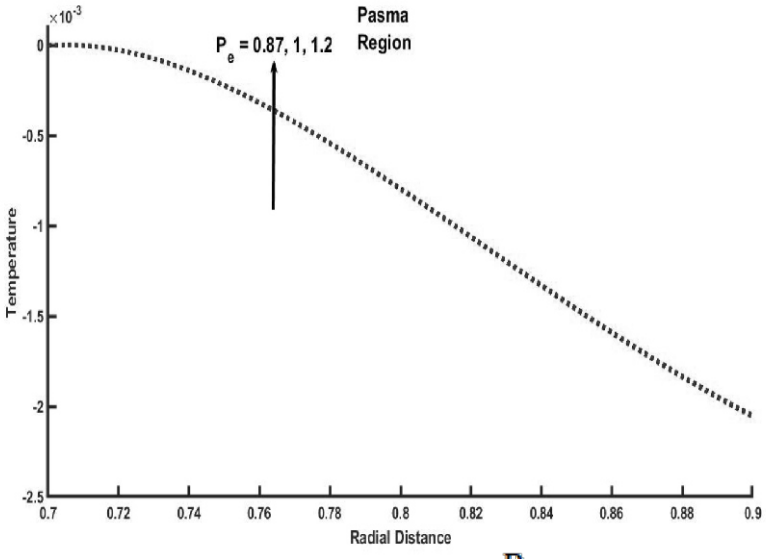

Fig. 9: Temperature for P_e.

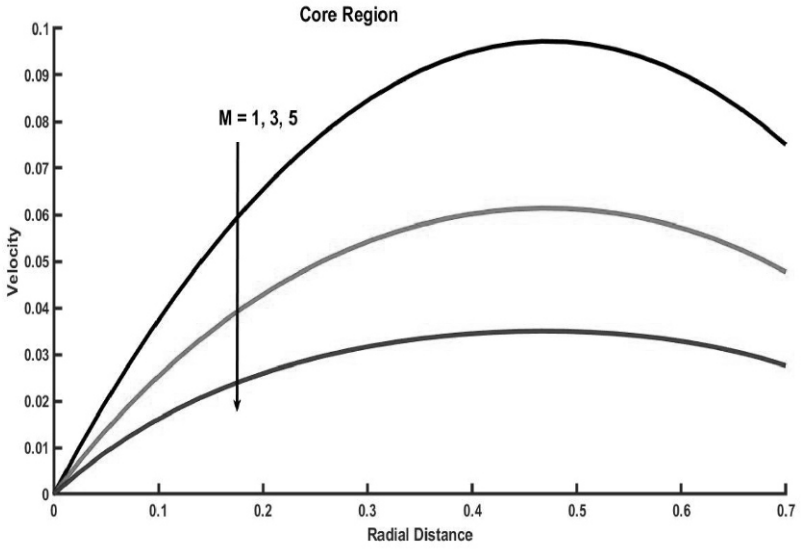

Fig. 10: Velocity for M.

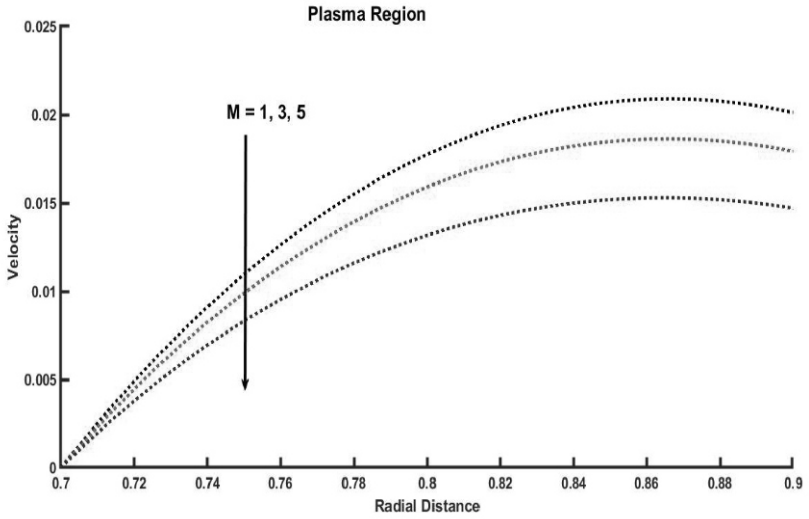

Fig. 11: Velocity for M.

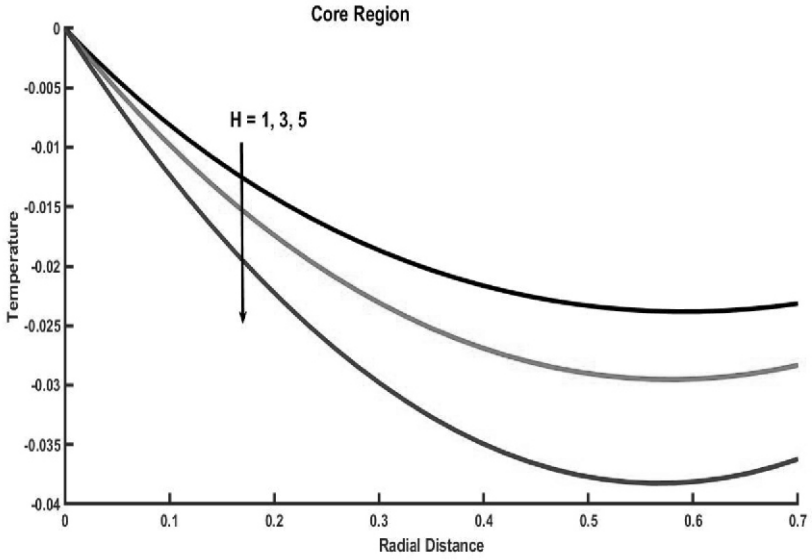

Fig. 12: Velocity for H.

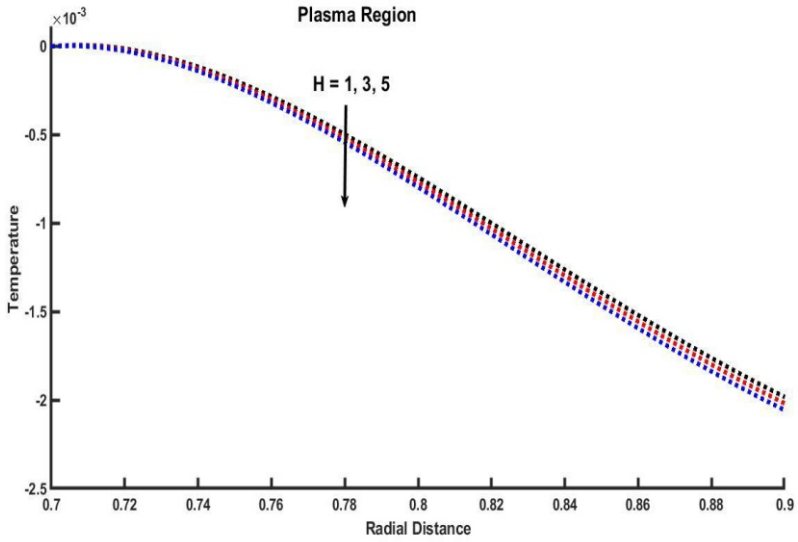

Fig. 13: Velocity for H.

Figures 6 & 7 include a discussion of the velocity with various values of the pressure gradient (P_0). These figures may be seen below. It can be observed that there is a opposite relationship among the pressure gradient and the velocity. These figures demonstrate an inverse correlation between pressure gradient and velocity. Figures 8 & 9 illustrate the temperature curve for a range of various Peclet numbers and their associated values. The Peclet number is dependent on the temperature, thus as it rises, therefore the temperature. The temperature is influenced by the Peclet number, with higher Peclet numbers corresponding to higher temperatures.

The fluctuation in the speed of the blood flow with different values of magnetic parameter which is shown in Figures 10 & 11. The graphic makes it clearly visible that there is a negative correlation between them. Physically, the Lorentz force, which functions as a resistive drag force, is responsible for this phenomenon. An activity that increases the internal viscosity of the fluid, which in turn makes it easier for red blood cells to remain suspended in the fluid. Consequently, the core and plasma areas both experience a reduction in velocity as a result of this. The variations of temperature distribution with respect to the heat production parameter is seen in From the Figures 12 & 13, it is clear from looking at the numbers that heat generation parameter tends to reduce the heat transfer process.

5. Conclusion

- Based on the graphic results, the following key conclusions can be drawn:
- Increased magnetic field strength leads to decreased velocity in both the central core and plasma areas, which holds potential implications for surgical procedures within the human body.
- The numerical findings underscore the sensitivity of two-phase fluid flow to both stenosis and magnetic fields.
- As the core layer thickens, the Reynolds number decreases, relating with increased resistance.
- Heat generation parameter tends to reduce the heat transfer process in both regions.
- Higher temperatures in both areas result from higher radiation parameters in stenosed arteries, suggesting potential applications in cancer treatment techniques such as hyperthermia.

REFERENCES:

- C. P. Granger, "Arterial blood flow dynamics and the effects of atherosclerosis," J. Vasc. Res., vol. 52, no. 2, pp. 111-123, 2015.
- S. S. Bhattacharya and M. P. K. Patra, "A review of hemodynamic factors in arterial stenosis," Int. J. Cardiol., vol. 200, pp. 199-208, 2015.
- T. F. L. Costa et al., "Hydrodynamic effects of stenosis in arterial blood flow," Biophys. J., vol. 108, no. 3, pp. 678-686, 2015.
- J. M. Clark, "Experimental studies on blood flow in stenotic arteries," Vasc. Med., vol. 20, no. 4, pp. 300-310, 2015.
- M. B. Al-Rashid et al., "The application of magnetic fields in blood flow studies," J. Biomech., vol. 49, no. 2, pp. 330-335, 2016.
- A. Tzirtzilikis, "Regulating bio-magnetic fluid circulation in narrowed pathways," J. Biomech., vol. 48, no. 7, pp. 1312-1321, 2016.
- R. Ponalagusamy and P. Selvi, "Influence of magnetic fields on two-phase blood flow," J. Fluid Mech., vol. 27, no. 1, pp. 83-92, 2016.
- L. R. Ali et al., "MHD blood flow modeling using Casson fluid," J. Magnetohydrodyn., vol. 52, no. 1, pp. 45-53, 2017.
- P. Majee and A. Shit, "Heat transfer effects on blood flow in stenosed arteries," J. Med. Phys., vol. 42, no. 2, pp. 175-181, 2017.
- K. H. Chen et al., "Temperature dependency of blood viscosity in two-phase models," J. Biomech., vol. 51, no. 6, pp. 1107-1113, 2018.
- N. K. S. Kumar et al., "Magnetohydrodynamic effects in blood flow," Int. J. Eng. Sci., vol. 139, pp. 165-175, 2018.
- A. R. Misra et al., "Modeling arterial blood flow as a conduit," Comput. Biol. Med., vol. 106, pp. 55-64, 2019.
- J. H. Liu et al., "Advanced imaging techniques for hemodynamic analysis," J. Vasc. Surg., vol. 69, no. 4, pp. 1300-1308, 2019.
- T. M. V. Quintana et al., "Computational fluid dynamics in arterial diseases," J. Biomech., vol. 92, pp. 106-116, 2019.
- M. Ikbal et al., "Flow properties of blood in two-phase models," Phys. Fluids, vol. 31, no. 12, pp. 122104, 2019.
- R. Ponalagusamy, "Comparative studies on blood flow dynamics," Appl. Math. Mech., vol. 40, no. 5, pp. 579-589, 2020.
- H. A. De Lima et al., "Influence of arterial geometry on blood flow," J. Biomech., vol. 106, pp. 45-53, 2020.
- P. T. V. Nguyen et al., "Effects of stenosis height on blood flow," J. Vasc. Res., vol. 57, no. 3, pp. 189-197, 2020.
- D. D. K. Joseph et al., "Impact of heat transfer in MHD blood flow," Thermal Sci., vol. 24, no. 5, pp. 301-310, 2020.
- M. E. U. Rahman et al., "Exploring two-phase flow in stenosed arteries," Biophys. J., vol. 119, no. 6, pp. 1234-1242, 2020.
- A. F. N. de Souza et al., "Magnetic field effects on blood viscosity," J. Biomech., vol. 102, pp. 123-130, 2021.
- S. H. Ali and M. A. K. Khan, "MHD modeling of blood flow: A review," J. Magnetohydrodyn., vol. 57, no. 1, pp. 15-22, 2021.
- I. B. M. P. Santos et al., "The role of temperature in blood flow," J. Therm. Biol., vol. 95, p. 102759, 2021.
- H. G. C. Leite et al., "Assessing two-fluid models in arterial flow," J. Biomech., vol. 132, pp. 104835, 2021.
- R. S. Z. G. Valenzuela et al., "Effects of stenosis on hemodynamics," J. Biomech., vol. 54, no. 5, pp. 789-796, 2021.
- J. E. C. Macedo et al., "Innovations in imaging for vascular studies," Radiology, vol. 299, no. 2, pp. 341-348, 2021.
- A. D. H. Fonseca et al., "Understanding flow dynamics in diseased arteries," Cardiovasc. Eng. Technol., vol. 12, no. 3, pp. 217-229, 2021.
- M. B. D. C. P. C. Marques et al., "Thermal management in MHD blood flow," J. Med. Phys., vol. 46, no. 4, pp. 300-308, 2021.
- T. H. S. Z. Santos et al., "Evaluating arterial disease and biomechanics," J. Vasc. Surg., vol. 74, no. 3, pp. 681-690, 2021.
- R. P. S. H. H. Rodrigues et al., "Advancements in treatments for arterial stenosis," J. Clin. Investig., vol. 131, no. 9, p. e14689, 2021.